Thin Solid Films 518 (2009) 1067–1071

Contents lists available at ScienceDirect

Thin Solid Films

journal homepage: www.elsevier.com/locate/tsf

Analysis of thermal effect on transparent conductive oxide thin films ablated by UV laser

Ming-Fei Chen [a,*], Yu-Sen Ho [a], Wen-Tse Hsiao [a], Kuo-Cheng Huang [b], Yu-Pin Chen [c]

[a] Department of Mechatronics Engineering, National Changhua University of Education, Changhua, 50007, Taiwan, ROC
[b] System Control and Integration Division, Instrument Technology Research Center, National Applied Research Laboratories, 20 R&D Road VI, Hsinchu Science Park, Hsinchu City, Taiwan, ROC
[c] PCB Department, Tongtai Machine & Tool Co., Ltd, Kaohsiung, 82151, Taiwan, ROC

ARTICLE INFO

Available online 16 September 2009

Keywords:
Heat affected zone
Electro-optical efficiency
Debris
Micro-crack
Temperature distribution

ABSTRACT

Transparent conductive oxide thin films are applied to many computer, communication and consumer electronics products including thin film transistor liquid crystal displays, organic light emitting diodes, solar cells, mobile phones, and digital cameras. The laser direct write patterning of the indium tin oxide (ITO) thin film processing technique produces a heat affected zone that has an enormous effect on the electro-optical efficiency of transparent conductive oxide films. This is because direct laser writing patterning in thermal machining process can create debris and micro-cracks in the substrate. Therefore, this study establishes the ultraviolet (UV) laser ablation of temperature model on the polycarbonate and soda-lime glass substrates using the finite element analysis software ANSYS, and measures the temperature field based on the laser micro-patterning process. The meshing model determines the structure of the pre-processors and parameters were set with ANSYS parameter design language. This study also simulates the Gaussian distribution laser irradiation on the pre-processor structure. A UV laser processing system made micro-patterning on ITO thin films to analyze which conditions damaged the substrates. Comparing the simulation and experiment results reveals the minimum laser ablation threshold of the ITO thin films with the melting and vaporization temperatures. Simulation results show that the temperature distribution on PC and soda-lime glass substrates after laser irradiation of 1.05 μs with a laser output power of 0.07 W produces temperatures of approximately 52 °C, 54 °C and 345°Cand 205 °C at the laser output power of 0.46 W. The experiment results show that the patterning region is similar to the simulation results, and the lower laser power does not damage the substrates.

1. Introduction

Laser processing technologies, such as drilling, welding, cutting, hardening, surface treatment and repairing, are widely used in the mechanical, photoelectronic, optical and electronic industries. Laser absorption, reflection and transparency can affect the laser irradiation of a material's surface. Therefore, when the absorbed energy is high enough, the surface of the material can melt and vaporize. This phenomenon occurs in many applications, including drilling microvia of high density interconnect structures, cutting steel slabs, optical plastic, and fiberglass, welding multi-components, hardening material surfaces, and surface treatment of optical components to increase efficiency.

Some investigations have been conducted on the laser material processing technology using different laser sources, analysis methods, and materials. Kang et al. [1] proposed a heat transfer and residual distortion analysis of a laser welding erbium doped fiber amplifier laser diode pump using the finite element method. In the Nd:YAG laser welding process, distortion happens at the ferrule and saddle during heating and cooling. Therefore, numerical analysis can be used to obtain optimization parameters and decreasing displacement [1]. Gordon et al. [2] provided a simulation tool for manufacturing and discussed the laser pulsed energy from 1 μJ to 300 μJ. Simulation of relationship between pulse energy, etch rate, pulse frequency, and preheating temperature of the substrates requires a minimum beam diameter of approximately 30 μm. The simulation and experiment results are in agreement. Wang and Lin (2007) used the commercial software ABAQUS to analyze a CO_2 laser source with a line-shaped beam to cleave soda-glass substrate. In their experiments they discussed various rotation angles of the line-shaped beam. Finally, they discovered that thermal diffusion and rotation angle cause the phenomenon of micro chip formation due to a large tensile stress inside the soda-glass substrates. Further, the rotation angle at 0° of the line-shaped beam causes a micro-crack effect. Yavas and Takai [3] utilized various laser sources of the fundamental and fourth harmonic generator Nd:YLF with wavelengths of 262 nm and 1047 nm to

* Corresponding author.
E-mail address: chenmf@cc.ncue.edu.tw (M.-F. Chen).

0040-6090/$ – see front matter © 2009 Published by Elsevier B.V.
doi:10.1016/j.tsf.2009.08.053

directly write on ITO thin films. Their experiments were carried out at high speed scribing of 1 m/s [3]. Li et al. proposed a laser micro-cladding technique applicable to manufacturing of electronic circuit conductors on Al_2O_3 substrate [4]. This method achieves a minimum linewidth of about 20 μm and a maximum linewidth of about 1 mm. This approach also has the advantages of low cost and rapid prototyping for high speed fabrication of print circuit boards [5]. Raciukaitis et al. [5] utilized a high repetition rate picosecond lasers to pattern indium–tin oxide films. They then analyzed the groove profiles with an optical microscope, stylus type profiler, scanning electron microscope, and atomic force microscope. The threshold of 266 nm and 355 nm wavelength radiation was about 0.20 J/cm^2 and 0.46 J/cm^2, respectively. In their study, the laser energy was 130 mW and 100 mW, the feeding speed 300 mm/s and 100 mm/s, and the minimum linewidth was 13 μm and 7 μm. It has been successful removing ITO thin films without damaging the structure [6]. The current study explores the temperature distribution of laser irradiation on PC and soda-lime glass substrates using commercial finite element analysis (FEA) software. Finally, this study also compares the simulation and experimental results.

2. Modeling of thermal analysis process

The finite element analysis method is a useful tool for computer-aided engineering analysis. This approach makes it easier to predict material types and manufacturing process parameters. Fig. 1 shows a flowchart of the temperature distribution prediction procedure using finite element simulation.

The thermal analysis of thin films and substrates usually assumes that the laser energy is a Gaussian distribution. The surface heat flux distribution $q(x,y)$ can be calculated according to Eq. (1) [7]:

$$q(x,y) = \frac{2\alpha P}{\pi r^2}\exp\left[\frac{-2(x^2+y^2)}{r^2}\right] \tag{1}$$

where α is the laser absorption coefficient of laser beam irradiation on the material surface, P is the laser beam power, and r is the laser beam radius. According to Fourier's law of heat conduction, the heat flux Φ, is directly proportional to the temperature gradient, as shown in Eq. (2) [8]:

$$\Phi(Z) = -k\left(\frac{dt}{dz}\right) \tag{2}$$

where k is the heat conduction coefficient, and Z is the surface depth of the material. The relationship between the heat conduction coefficient and the heat diffusion coefficient can be calculated by Eq. (3) [8]:

$$k_d = \frac{k}{\rho C_p} \tag{3}$$

Table 1
Physical parameters of polycarbonate substrate in simulation [9–13].

Properties	Polycarbonate (PC)
Density (kg/m^3)	1250
Heat capacity (J/kgK)	1200
Thermal conductivity (W/mK)	0.2

where k_d is the thermal diffusivity, ρ is the energy density of laser, and C_p is the specific heat.

Using the laser beam to produce heat energy, Fourier's thermal differential equation can be obtained from Eq. (4) [7]:

$$\frac{\partial T}{\partial t} = k_d\nabla^2 T + \frac{q(x)}{\rho C_p}. \tag{4}$$

Substituting expressions (1) and (3) into Eq. (4) makes it possible to obtain the surface temperature of materials, as expressed in Eq. (5) [8]:

$$T = \frac{2(1-r)\rho}{k}\sqrt{\frac{k_d t}{\pi}} \tag{5}$$

where $(1-r)$ is absorption of the materials, ρ is the power density of the laser, and T is the temperature at the surface of the irradiated target.

3. Numerical simulation process

The finite element model in this study uses in real specimens, 20 mm×20 mm×1.1 mm for the soda-glass specimen and 20 mm×20 mm×1 mm for the polycarbonate specimens, respectively. The sample was irradiated by a UV laser beam. Before establishing the mathematical modeling, some assumptions must be made: (1) Thermal convection and radiation are neglected during the heating process. (2) The thermal properties are isotropic. (3) Latent heat is neglected during the heating process. (4) The laser intensity distribution is an ideal Gaussian (TEM_{00}) mode. (5) There is no phase change during laser heating.

The physical parameters for both ITO/glass and ITO/PC specimens for the mathematical model and temperature distribution can be calculated by ANSYS finite element analysis (FEA) software. Table 1 shows the physical parameters of the specimens used in the simulations [9–13]. Eq. (6) shows that the absorption is calculated as follows.

$$A = 1 - R - T \tag{6}$$

where A, R, and T represent absorptance, reflectance, and transmittance.

The solution processes use the following boundary conditions and material loads. An initial temperature of 27 °C, laser irradiation time of

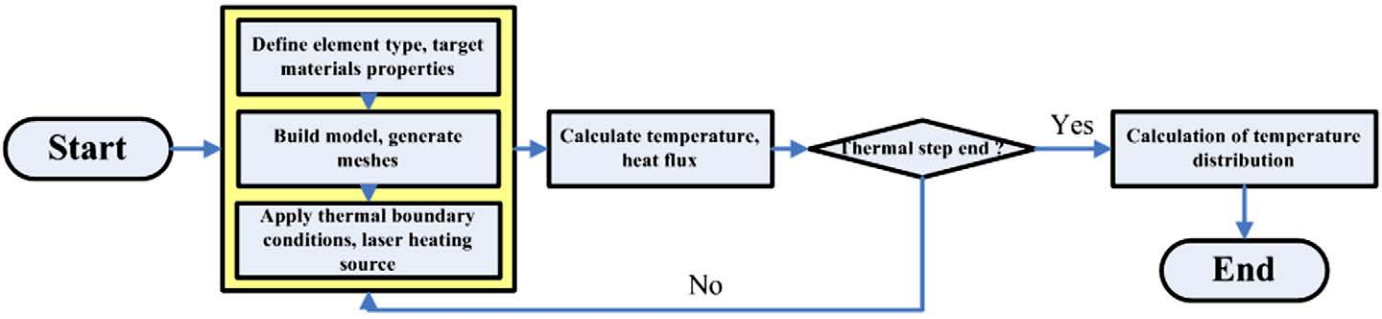

Fig. 1. Flowchart of the temperature distribution prediction procedure.

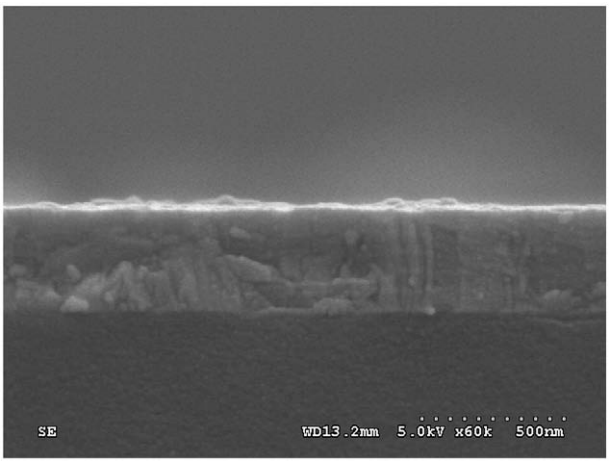

Fig.2. SEM morphology of cross-section of ITO films deposited on soda-lime substrates.

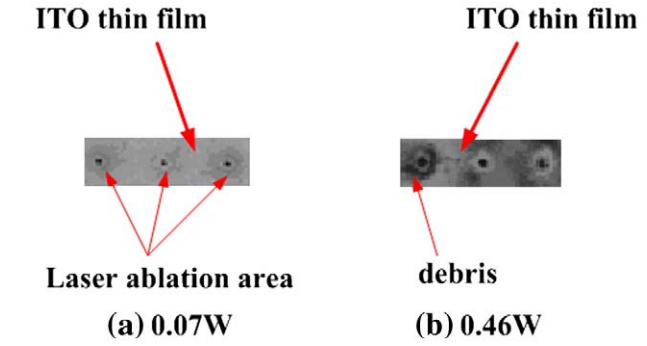

Fig. 4. Optical microscope of laser ablation and untreated regions on ITO/glass substrates.

1.05 μs, and a function-editor were employed to define the Gaussian irradiation heating source.

4. Results and discussion

4.1. Experimental results

ITO thin film patterning in this study uses Nd:YAG laser source with third harmonic generator settings to produce ITO/PC and ITO/glass structures. The experimental specimens are soda-lime glass and polycarbonate substrates with a commercial ITO thin film 400 nm thick. SEM morphology of cross-section of ITO films deposited on soda-lime substrates was inspected with a field emission scanning electron microscope as shown in Fig. 2. The dimension of the each specimen is 10 mm^2. Before laser patterning, the specimen was cleaned in an ultrasonic bath with liquid alcohol, and dried under high pressure nitrogen gas. The laser operating parameters include a TEM_{00} Gaussian distribution, pulse repetition frequency of 8 kHz, pulse width of 35 ns, and wavelength of 355 nm. Fig. 3 shows the different laser power ablation of ITO films on the polycarbonate plastic material. Fig. 3(a) shows the experimental results for a laser power of 0.07 W and heating duration of 1.05 μs. Fig. 3(b) shows the results for a 0.46 W laser power for the same heating duration. Fig. 4 shows the different laser power ablations of ITO films on the glass substrate. The ablation of the ITO/glass substrate shows more burning and debris when the laser power is 0.46 W than when it is 0.07 W. In order to check the electric isolation of conductive films, the removal region and non-removal region were measured by multimeter. After laser irradiation, the electric insulation region was successful in the above cases. A laser power of 0.46 W does not cause micro-cracks in the glass substrate. However, a large spatter region on the substrate surface affects transmission efficiency.

4.2. Case I—thermal analysis of polycarbonate (PC) substrate

This study experimentally determines the reflectance and transmittance data of the PC and soda-lime glass substrates by spectrophotometry (Lambda 900, UV/Vis/NIR spectrophotometer system). Fig. 5 shows the transmittance and reflectance spectra data of the polycarbonate substrates. From Fig. 5, these results show that reflectivity from ultraviolet to infrared of about 10%. Moreover, the transmittance in the visible range (400 nm–800 nm) approximates 90%. The spectrophotometer measures the polycarbonate substrate with a laser wavelength of 355 nm, revealing a transmittance of about 50.6% and reflectance of 13.0%. In addition, the optical transmission spectra at IR range displays a strong absorption caused by adsorbed water vapor [15,16]. Substituting these two parameters into Eq. (6) shows that the absorptance amount is 36.4%. Prior to simulation, the substrate material was assumed to be at constant ambient temperature which the units as centigrade (i.e., $T_{int} = 27$ °C). Fig. 6(a) and (b) display cross-sections of the temperature distribution with 1.05 μs laser irradiation at a laser output power of 0.07 W and 0.46 W, respectively. Fig. 6(a) shows that the center maximum temperature of the spot reaches 52 °C. For the same condition, when the laser output power increases to 0.46 W, the maximum surface temperature reaches 345 °C. This proves that the temperature distribution of the surface and interior structure exceeds the melting point of 130 °C [14], as Fig. 6(b) shows. This means that laser irradiation on the specimens could damage the polycarbonate structure at high temperature.

4.3. Case II—thermal analysis of glass substrate

This study measures the optical properties of soda-lime glass substrates using a spectrophotometer. Fig. 7 shows the optical transmittance

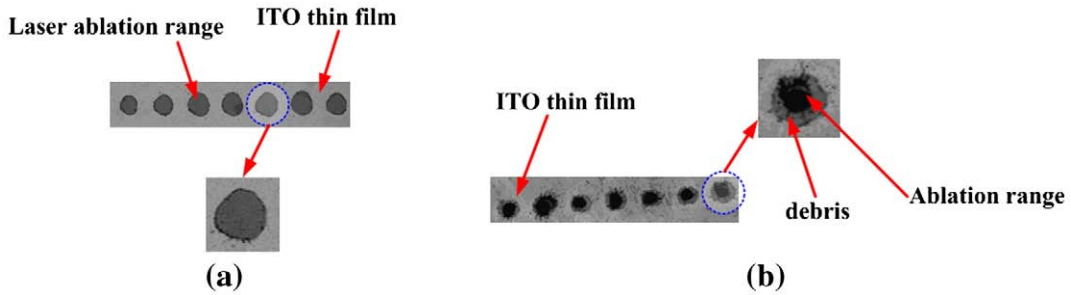

Fig. 3. Optical microscope of laser ablation and untreated regions on ITO/PC substrates (a) 0.07 W and (b) 0.46 W.

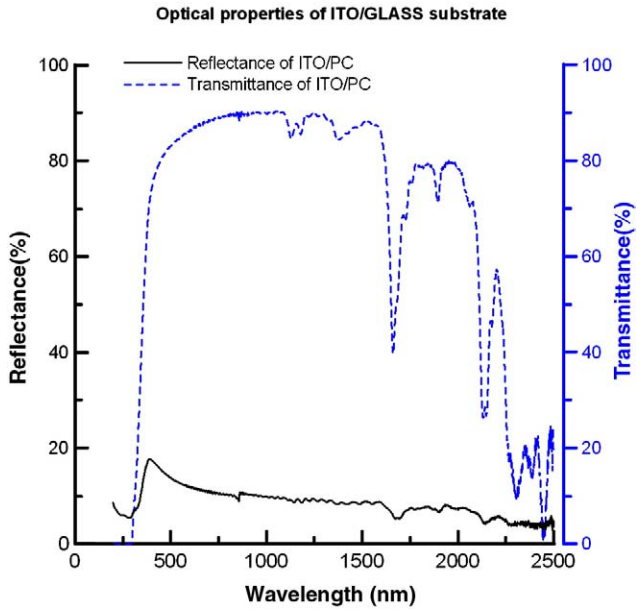

Fig. 5. Optical reflectance and transmittance versus wavelength for polycarbonate substrates.

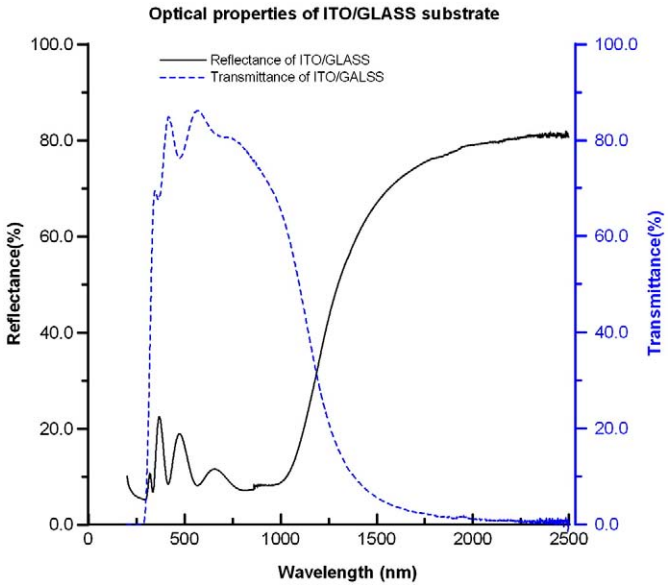

Fig. 7. Optical reflectance and transmittance versus wavelength for soda-lime glass substrates.

and reflectance data of the soda-lime glass substrate. These results show that reflectivity increases as the wavelength increases. In this case study, the transmittance is 68.4% and reflectance is 18.4%. Before simulation, the constant temperature boundary was assumed ($T_{int} = 27$ °C) whose unit was the centigrade. Fig. 8 shows the temperature distribution during the laser beam ablation of ITO/glass substrates after laser irradiation. Fig. 8(a) displays the cross-section of the temperature distribution at a laser output power of 0.07 W and laser irradiation of 1.05 μs. This figure shows that the maximum center surface temperature is 54 °C, which means that the heating influence does not damage the substrate. Fig. 8(b) shows a cross-section of the temperature distribution for a laser output power of 0.46 W and laser irradiation time of 1.05 μs. This case study shows that the center maximum temperature of the substrate reaches about 205 °C, which is much less than the substrate's melting temperature of 820 °C.

5. Conclusions

Using the numerical analysis method and the FEA software ANSYS, the physical and optical parameters of the ITO/PC and ITO/glass substrates can be used to evaluate the thermal affect and thermal distribution. This study also discusses the maximum temperature distribution of the laser ablation rate relationship for the melting between the vaporization. Finally, the experimental results and numerical analysis in this study present ITO/PC and ITO/glass substrates to further improve laser ablation on different materials.

Acknowledgement

The authors would like to thank the National Science Council of the Republic of China, Taiwan for financially supporting this research under Contract No. NSC 97-2221-E-018-007-MY2.

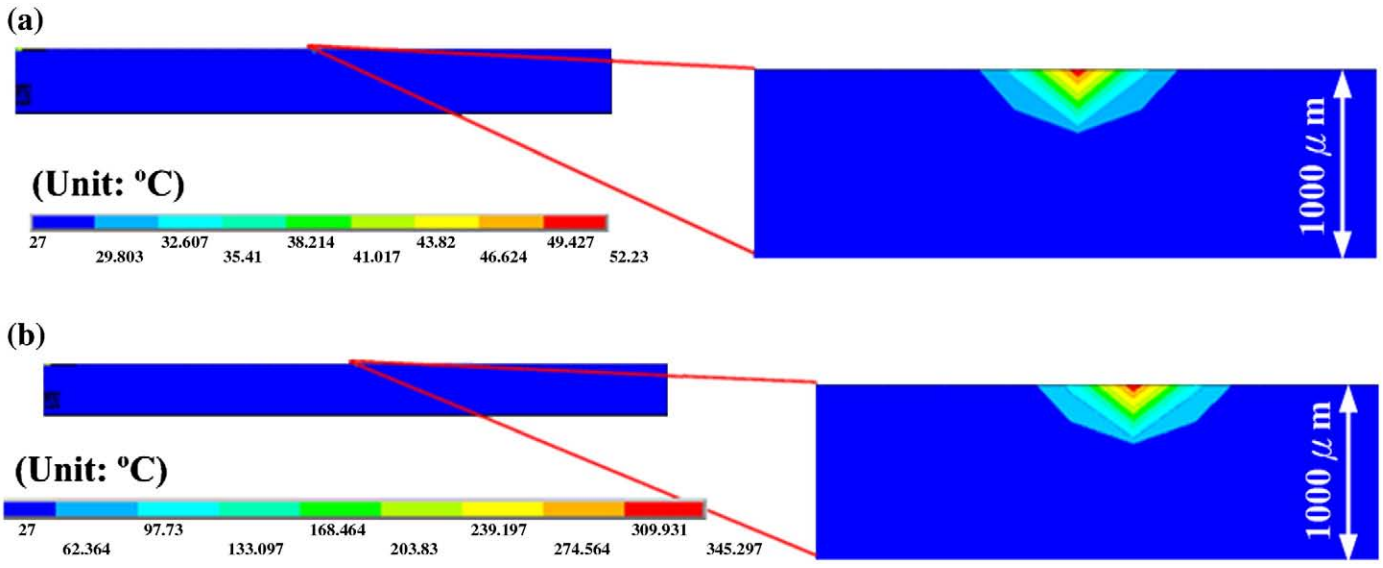

Fig. 6. Temperature distribution during laser ablation on ITO/PC substrate. (a) Temperature distribution of laser power of 0.07 W, and (b) 0.46 W after laser irradiation of 1.05 μs.

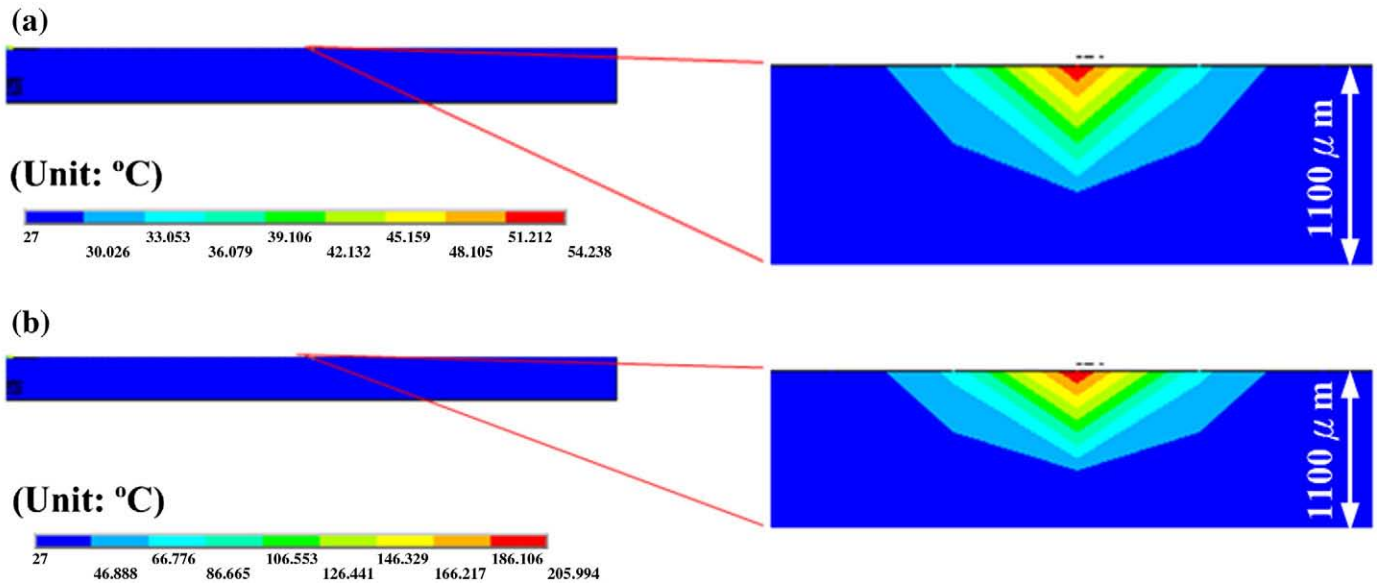

Fig. 8. Temperature distribution during laser ablation ITO/glass substrate. (a) Temperature distribution of laser power of 0.07 W and (b) 0.46 W after laser irradiation of 1.05 μs.

References

[1] D.H. Kang, K.J. Son, Y.S. Yang, Finite Elem. Anal. 37 (2001) 749.
[2] P. Gordon, B. Balogh, B. Sinkovics, Microelectron. Reliab. 47 (2007) 347.
[3] O. Yavas, M. Takai, Appl. Phys. Lett. 73 (1998) 2558.
[4] X. Li, H. Li, Y. Chen, X. Zeng, Appl. Phys., A 79 (2004) 1861.
[5] G. Raciukaitis, M. Brikas, M. Gedvilas, T. Rakickas, Appl. Surf. Sci. 253 (2007) 6570.
[6] A. Buz'as, Z. Geretovszky, Thin Soild Films 515 (2007) 8495.
[7] M. Von Allmen, Laser-Beam Interactions with Materials, Springer-Verlag, Berlin, 1995.
[8] F.P. Incropera, D.P. DeWitt, Fundamentals of Heat and Mass Transfer, John Wiley & Sons, New-York NY, 1985.
[9] D.R. Dance, C.L. Skinner, K.C. Young, J.R. Beckett, C.J. Kotre, Phys. Med. Biol. 45 (2000) 3225.
[10] H. Becker, U. Heim, Sens. Actuators, A 83 (2000) 130.
[11] X. Zhang, W. Hendro, M. Fujii, T. Tomimura, N. Imaishi, Int. J. Therm. 23 (2002) 1077.
[12] L. Jakevičius, J. Butkus, A. Vladišauskas, ULTRAGARSAS 55 (2005) 17.
[13] P.B. Narottam, R.H. Doremus, Handbook of Glass Properties, Academic Press, New York NY, 1986.
[14] S. Bäumer, Handbook of Plastic Optics, WILEY-VCH Verlag GmbH & Co. KGaA, Weinheim, 2005.
[15] W.F. Wu, B.S Chiou, Thin solid Films 298 (1997) 221.
[16] N. Al-Dahoudi, H. Bisht, C. Gobbert, T. Krajewski, M.A. Aegerter, Thin Solid films 392 (2001) 299.